Spatio-temporal analysis of land use/land cover change dynamics in Paraguai/Jauquara Basin, Brazil

Daniela Silva [a,*], Edinéia A. S. Galvanin [b], Raquel Menezes [c]

[a]*Department of Mathematics, Center of Mathematics, Minho University, Gualtar, 4710-057 Braga, Portugal*
[b]*Department of Geography, São Paulo State University, Ourinhos 19901-700, São Paulo, Brazil*
[c]*Department of Mathematics, Center of Mathematics, Minho University, Azurém, 4800-058 Guimarães, Portugal*

Abstract

Although global climate change is receiving considerable attention, the loss of biodiversity worldwide continues. In this study, we investigated the dynamics of land use/land cover (LULC) change in the Paraguai/Jauquara Basin, Mato Grosso, Brazil. Two analyses were performed using R software. The first was a comparative study of LULC among the LULC classes at the polygon scale, and the second was a spatio-temporal analysis of moving polygons restricted to the agricultural regions in terms of topology, size, distance, and direction of change. The data consisted of Landsat images captured in 1993, 1997, 2001, 2005, 2009, 2013, and 2016, and processed using ArcGIS software. The proposed analytical approach handled complex data structures and allowed for a deeper understanding of LULC change over time. The results showed that there was a statistically significant change from regions of natural vegetation to pastures, agricultural regions, and land for other uses, accompanied by a significant trend of expansion of agricultural regions, appearing to stabilize from 2005. Furthermore, different patterns of LULC change were found according to soil type and elevation. In particular, the purple latosol soil type presented the highest expansion indexes since 2001, and the elevated agricultural areas have been expanding and/or stabilizing since 1997.

Keywords: LULC, Spatio-temporal pattern, Moving polygon analysis, Spatial autocorrelation, Remote Sensing, Anthropogenic activities

Declarations

Conflicts of interest/Competing interests: Daniela Silva, Edinéia A. S. Galvanin, and Raquel Menezes declare that they have no conflict of interest.
Availability of data and material: Data was collected from freely available images composites from the catalogs of the United States Geological Survey.
Code availability: QGIS software (version 2.14.21), Geo-reference Information Processing System (SPRING) (version 5.5.2), ArcGIS (version 9.2), and RStudio software (version 1.2.5033).

Acknowledgements

This work is part of the results of the research projects *PTDC/MAT-STA/28243/2017* funded by the FCT (Fundação para a Ciência e Tecnologia) and *Análise temporal do uso da terra para definição de cenários de mudança da paisagem natural por intervenções de natureza humana no Pantanal de Cáceres/MT* funded by Fundação de Amparo à Pesquisa do Estado de Mato Grosso-FAPEMAT. The first author also acknowledges Foundation FCT (Fundação para a Ciência e Tecnologia) for funding this research through Individual Scholarship Ph.D. PD/BD/150535/2019.

*Corresponding author
Email address: `danyelasylva2@gmail.com` (Daniela Silva)

1. Introduction

Over the last decades , tropical forests have been significantly degraded and destroyed by anthropogenic activities. Deforestation destroys the natural habitat and, consequently, leads to a decline in biodiversity. It can also result in forest fragmentation, which can result in areas that are too small for some species to survive or in large distances between species. Therefore, a long process of decay in residual diversity is observed (Morris, 2010), and land management becomes one of the most important factors influencing the supply of ecosystem services (van Oudenhoven et al., 2012).

In short, human activities make use of natural resources, and this impacts ecological processes and functions. This is known as land use (Veldkamp and Fresco, 1996). Information about land cover is essential for the planning and management of natural resources (Zhu, 1997). Thus, the analysis of ecosystem changes, particularly land use/land cover (LULC) change, has become relevant during the process of land management decision-making. Such changes can include losses of forest, water bodies, agricultural areas, and other vegetated green spaces. Detecting change dynamics has attracted great attention (Lu et al., 2013); however, it faces some challenges.

Although many change detection methods have been developed, most are only used to detect binary change and non-change categories (Lu et al., 2004). According to Mizutani and Murayama (2011), the major data formats used to represent LULC are the raster format and polygon-based formats. While in raster-based LULC data each location has an individual value and is described pixel by pixel, in polygon-based LULC data homogeneous space is defined as one polygon. Polygon representation is the most useful since it is the only one that can fully contain all geometric information, and it may consider polygon adjacency and topological relationships, which are important features for understanding LULC change (French and Li, 2010). Polygon-based data can also permit LULC fragmentation analysis; this is important for assessing how anthropogenic and natural factors can influence LULC changes (Lu et al., 2013).

Methods based on the polygon format to study LULC change have been proposed. To explain how societal and natural systems are affected by landscape changes, Sohl et al. (2019) applied a unique parcel-based modeling framework to produce high-resolution landscape projections at a national scale, the "Land Change Monitoring, Assessment, and Projection". Jacobson et al. (2015) introduced a method for accessing localized information in developing countries called GE Grids. This method is used to identify anthropogenic land conversion across East Africa and compare this against available land cover datasets through an interactive user-specified binary grid laid over Google Earth's high-resolution imagery. Galvanin et al. (2019) proposed a mixed-effects modeling approach for analyzing LULC change in the Brazilian Pantanal subregions of Cáceres, Mato Grosso State, Brazil. The models allow analysis of complex data structures and incorporate both fixed effects, associated with observed covariates, and random effects, which consider the particularities of each LULC class dependent on the year of data collection. Lu et al. (2013) provided a comparative analysis of LULC changes in the Brazilian Amazon at multiple scales, including per pixel, polygon, and census sector. Their research highlighted the necessity to implement change detection at multiple scales to understand LULC change patterns. Williams and Wentz (2008) proposed the TOSS method to understand LULC patterns. This method is used to examine whether similar geographic areas exhibit specific spatial patterns using additional attributes of polygons, such as type, orientation, size, and shape. Groups of similar regions are then created based on these attributes using cluster analysis, and the nearest neighbor analysis is used to compute the spatial distributions for each group.

Land use change modeling can be very challenging, and other advances have been made, such as the approaches presented by Gao and O'Neill (2019) and Verweij et al. (2018). Gao and O'Neill (2019) took a data-driven approach to develop a long-term spatially explicit urban land change model. The estimation process for each grid cell includes the capture of both the average grid-cell-level trajectory of land development applicable to all global grid cells and the local variations in the process of built-up land conversion across the world. The model incorporates the residuals resulting from both. Verweij et al. (2018) presented a new version of the CLUE model, the iCLUE model. This version incorporates solutions that address CLUE model issues, such as the process being time consuming and not producing self-explanatory results, and other issues directly related to the software. Both methods present good results, but they cannot be applied to the polygon data format, the importance of which has already been discussed. Very recently, Machado et al. (2020) introduced the LDTtool, a toolbox designed to assess landscape dynamics. The LDT method requires binary landscapes; as such, the area of interest must contain only one class of polygon, and it compares two metrics from two dates: the area and the number of patches. Although this method provides a diagnostic analysis and designs a future pattern, it works better in situations where there is little human interference (Machado et al., 2020).

Spatial dependency gives us information on spatial patterns, structures, and processes. Overmars et al. (2003) studied the spatial autocorrelation in LULC data from Ecuador. Since the analyzed LULC indicators were continuous, Moran's I was applied to study spatial dependency. In many LULC studies, the variable of interest is a factor, and Moran's I cannot be used. For this purpose, a join count test was developed, and it is not only used for binary data but can also be applied to multi-categorical data (Cliff and Ord, 1981). Mizutani and Murayama (2011) established an analytical framework for polygon-based studies of LULC change by defining polygon event and polygon state. Polygon event is related to changes in shape and attributes, while polygon state considers the spatial continuity and adjacency during the process. In particular, the combination of polygon events constitutes the change in polygon distributions (Sadahiro and Umemura, 2001), where events (such as stable, expansion, convergence, and division) characterize the change patterns based on a combination of the shape and the attributes. However, a more specific classification of changes can be considered, particularly the one proposed by Robertson et al. (2007).

The two main objectives of this study were (i) to compare and analyze the evolution of LULC for different LULC classes in the Paraguai/Jauquara Basin (BHPJ) and (ii) to study the spatial pattern, structure, and processes of changes in agricultural regions in the Bugres River Basin (BHRB). The ideas proposed here are illustrated with these two case studies, BHPJ and BHRB, but they can be easily applied to similar studies.

2. Methods

2.1. Study area

The BHPJ territory covers 16,482 km^2 and is located in the Brazilian area of the north-eastern Upper Paraguay Basin (BAP), in the central-west region of Brazil (Figure 1). The BHPJ area includes the Cerrado, Amazon, and Pantanal biomes, which are predominately savanna and seasonal forest (Brasil. Ministério do Meio Ambiente e Instituto Brasileiro de Geografia – IBGE, 2004; IBGE, 2012).

According to the Köppen classification, the region has a Cwa climate (tropical climate), and it has two well-defined seasons: the rainy season in the summer and the dry season in the winter (Fenner et al., 2014). The mean monthly temperature ranges from 23.0^{o}C to 26.84^{o}C, and total annual rainfall ranges from 1,200 to 2,000 mm (Souza et al., 2013).

The Serra das Araras Ecological Station is a conservation unit integral to the protection of nature that extends for 271 km^2 of the Cerrado biome, present relief dissected , with elevations above 700m. It is located in the southwest region of the BHPJ, with a mountain corridor connecting the Amazonian and Pantanal biomes (Brasil, 1982). It contains the Umutina Indigenous Land, an area of 28,120 hectares located between the municipalities of Barra do Bugres and Alto Paraguai (ISA, 2018; Monzilar, 2018). The source of the Paraguay River is located in the northeast region of the BHPJ; this is an important contributor to the flood pulse of the Pantanal.

According to Opršal et al. (2016), soil type may influence LULC changes. In addition to soil characteristics, elevation is a significant biophysical factor in agricultural land change since most cultivated lands are situated at lower elevations (Warra et al., 2015). Elevation can influence other factors that contribute to agricultural occupation, such as soil quality, land accessibility, and the capacity to use modern mechanical equipment (Opršal et al., 2016).

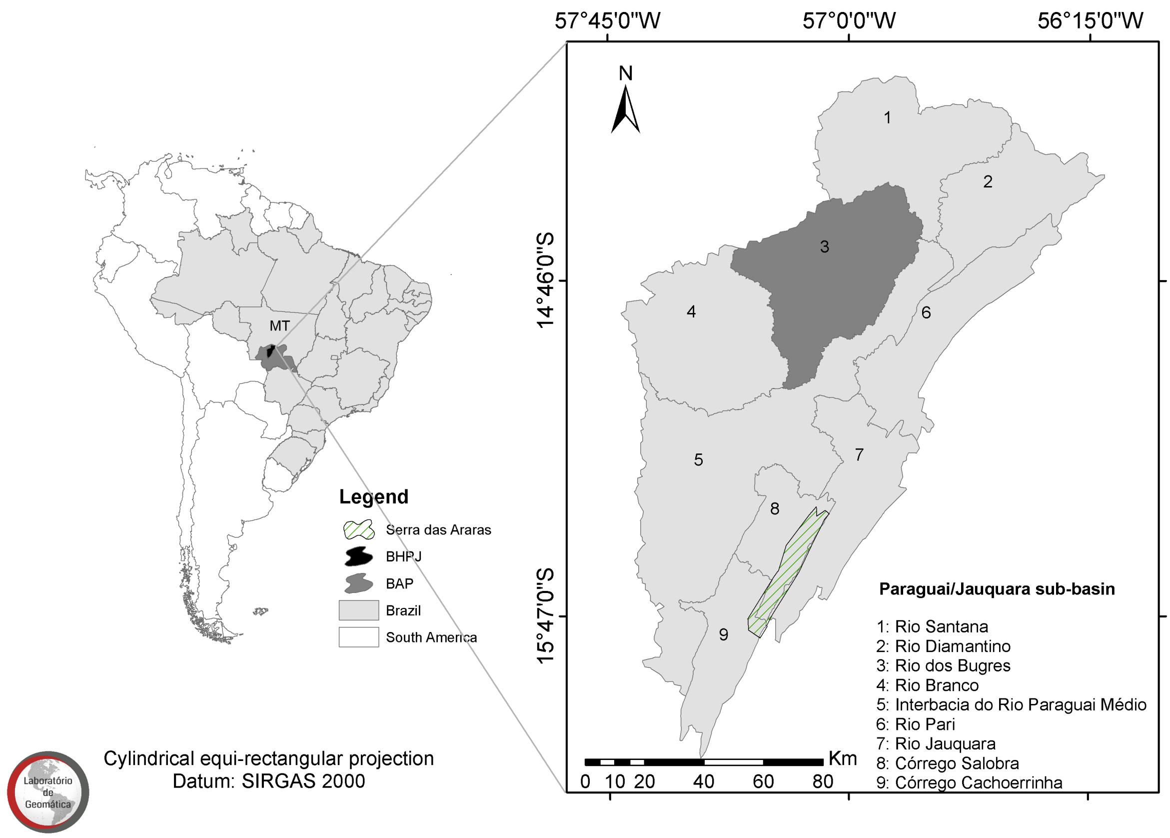

Figure 1: Map of BHPJ, Mato Grosso State, Brazil. On the right map, area 3 marked in dark-grey identifies BHRB.

2.2. *Data pre-processing*

A spatio-temporal analysis was used to study the LULC change in the BHPJ, Mato Grosso, Brazil. The methodology flowchart is presented in Figure 2.

Spatio-temporal data were collected to extract the LULC information. Image composites from the Thematic Mapper (TM) sensor onboard Landsat-5 (bands 3, 4, and 5) and the Operational Land Imager (OLI) sensor onboard Landsat-8 (bands 4, 5, and 6) were obtained; both were freely available from the image catalogs of the United States Geological Survey (USGS, 2017).

The BHPJ was covered by the Landsat scenes (path: 227; rows: 70 and 71) (30-m spatial resolution; 185-km swath width; 16-day temporal resolution; and 8-bit or 16-bit radiometric resolutions) (USGS, 2017). The images were captured in 1993, 1997, 2001, 2005, 2009, 2013 (Landsat-5, overpass: September), and 2016 (Landsat-8, overpass: August). Both August and September are in the dry period.

The delimitation of the BHPJ and BHRB was performed with the Digital Elevation Model from the Shuttle Radar Topography Mission (SRTM), with a spatial resolution of 30m, adapted for the Datum SIRGAS 2000, using the QGIS software (version 2.14.21) (QGIS Development Team, 2016).

The Landsat-5 images were geo-referenced using the Geo-reference Information Processing System (SPRING) (version 5.5.2) (Câmara et al., 1996) with Landsat-8 images as reference and a minimum error tolerance of 0.5 per pixel. ArcGIS (version 9.2) (ESRI, 2011) was used by radiometric correction. The mosaic of the images obtained by Landsat-5 and -8 and the geo-referenced images were imported into the Geo-reference Information Processing System (Câmara et al., 1996).

Landsat images were processed using the region growth algorithm available in the SPRING software. The best combinations for grouping two spectrally similar regions into a single region were: similarity value 10 and area 16 (1.44 hectare) for 1993, 1997, 2001, 2005, 2009 and 2013 images; and similarity value 10 and area 20 (1.8 hectare) for 2016 images.

Five thematic classes were considered based on the LULC classes proposed by IBGE (2013): pasture (grassland composed of cultivated pastures); natural vegetation (savanna and seasonal forest); agriculture

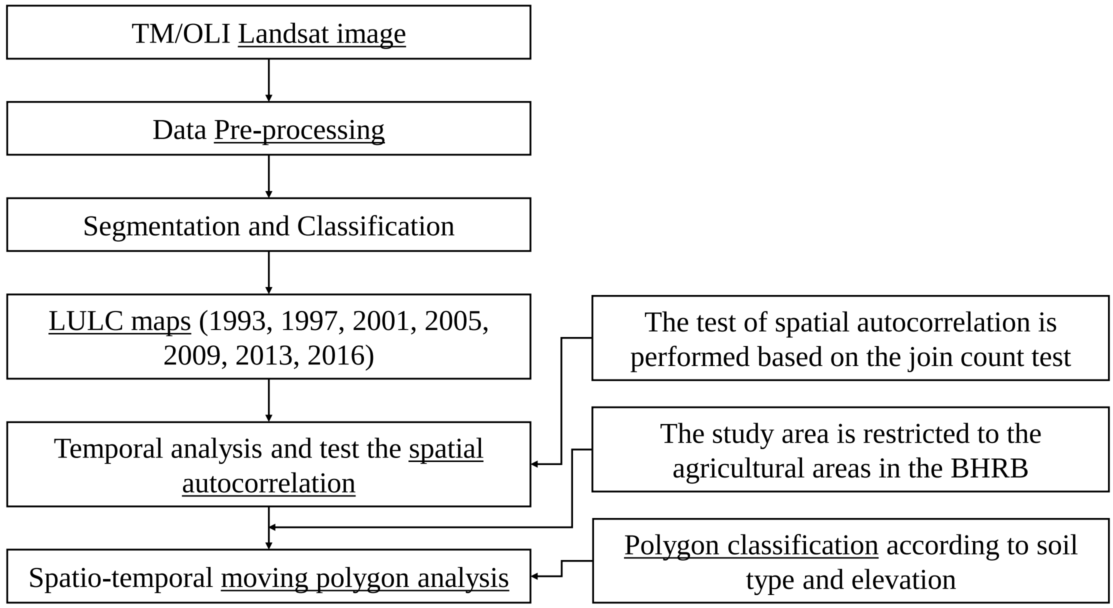

Figure 2: Methodology flowchart.

(all types of agricultural crops); water (all water bodies); and other uses (urban areas, farmhouses, roads, civil constructions, and mining).

The class training samples were identified, and the classification was supervised using Bhattacharya's method, which was performed in SPRING with a threshold of acceptance of 95% (Xaud and Epiphanio, 2014). The maps generated by SPRING were converted to matrix-vector form and exported in a shape file format to ArcGIS for cartographic mapping and quantification of thematic classes.

2.3. *Spatio-temporal analysis*

The spatio-temporal analysis was split into two steps. First, an exploratory method was used to analyze LULC changes at the polygon scale in the BHPJ, and this included a spatial autocorrelation analysis. Second, the area of interest was restricted to the BHRB, the area with more agricultural regions of the BHPJ. This second part consisted of a detailed spatio-temporal moving analysis of agricultural land use polygons in terms of topology, size, distance, and direction of change.

All analyses were performed using RStudio statistical software version 1.2.5033 (RStudio Team, 2019). The *spdep* package (Bivand, 2020) was used to study the spatial autocorrelation, while the *stampr* package was used for the spatio-temporal moving analysis (Long and Robertson, 2018).

The analyzed geodata consisted of polygons, each identified by: year of data collection (seven distinct years); area of the polygon (in hectares); LULC class (five classes); and geographical area of the region of interest (four classes: northwest, northeast, southwest, and southeast). Note that different representations of polygons were considered for the two data sets used in this study. For the BHPJ data, the polygon was identified by a pair of coordinates, while for the BHRB data, each polygon had defined boundaries determined by the LULC class.

2.3.1. *Spatial autocorrelation*

Spatial autocorrelation represents the relationship between nearby spatial units, where each unit has a realization of a single associated variable. In fact, the concept of spatial autocorrelation can be adopted in different situations. It can be used as a test for model mis-specification, a measure of the strength of the spatial effects on any variable, a means of identifying spatial clusters, a test for hypotheses about spatial relationships, and for other purposes. Examples of applications are reported by Getis (2010); Garcia-Soidan and Menezes (2012); Menezes et al. (2016).

In the current study, the spatial units were polygons, and the presence of spatial autocorrelation among realizations of the variable of interest, LULC class, was tested. Therefore, to assess the degree of clustering and dispersion of each LULC class, the joint count statistics test was used, with the assumption of independence between sampling outcomes and each locality.

The test statistic is given by the standardized normal statistic of the number of same-color joins (also denoted by Black-Black [BB] joins), testing whether they occurred more frequently than would be expected if the zones were labeled in a spatially random way (Cliff and Ord, 1981; Sokal and Oden, 1978). The spatial weights used were binary and retained a weight of unit for each neighbor relationship. On the other hand, the neighborhood was defined according to the k-nearest neighbor method, which involved finding, for each spatial unit, the closest group of k objects in terms of the Eucledian distance. The choice of k was based on a thumb rule, the square root of the data set dimension.

2.3.2. Spatio-temporal moving polygon

Spatio-temporal moving polygon analysis started with a categorization of polygon movement events based on the intersection of polygons from two different time stamps, and a distance threshold was used to verify whether the polygons were related between the time stamps. This categorization was performed with a hierarchical system (Robertson et al., 2007):

- Level 1 - stable (STBL), generation (GENR), and disappearance (DISA);
- Level 2 - STBL, GENR, DISA, expansion (EXPN), and contraction (CONT);
- Level 3 - STBL, GENR, DISA, EXPN, CONT, displacement (DISP), convergence (CONV), concentration (CONC), fragmentation (FRAG), and divergence (DIVR).

According to Robertson et al. (2007), this approach requires two assumptions: only unmovable polygons can be considered, and polygon changes are discontinuous. In the present case, both were verified since the agricultural regions were not movable objects and the observed time was discrete. Furthermore, the polygon events were classified based on combinations of change in shape and LULC class.

To compare different periods, the ratio and area of the observed events may be used (Sadahiro and Umemura, 2001; Mizutani and Murayama, 2011). However, the size measures only provide information about local changes in the sizes of temporally related polygons. In addition to the ratio and the size of events, other spatial properties associated with polygons may be taken into account, such as distance and direction, which may show the spatial relationships of polygons. In particular, the combination of local size changes with measures of direction can provide a metric and topological description of the characteristics of local change (Robertson et al., 2007).

Methods for quantifying distance relationships in polygon sets are well developed, and the calculation can be relatively straightforward. For this purpose, the Hausdorff distance may be adopted, which can be described as the maximum distance separating two polygons; that is, it measures the degree of mismatch between two polygons (Shao et al., 2010). The choice of the Hausdorff distance is justified by its greater sensitivity to changes in shape when compared to the centroid distance. Hence, the Hausdorff distance was used to quantify the distance between a polygon observed in a specific year and in the following year.

Conversely, there are many methods for performing polygon direction analysis. In this study, the simplest and most straightforward method was used—the centroid angle method. It measures the angle between two polygon centroids.

For this analysis, the study area was restricted to the agricultural areas of the BHRB due to the clear increases in these regions over time. Furthermore, after the categorization of polygon movement events, the soil type and elevation data were obtained for each area corresponding to each topological event. Soil type was classified into three categories: purple latosol (PL), red-yellow podzolic (RP), and red-yellow latosol (RL). PL soil is characterized by its great agricultural potential; it has higher fertility than the remaining latosols. RL soil has the largest and widest geographic distribution in Brazil, although it

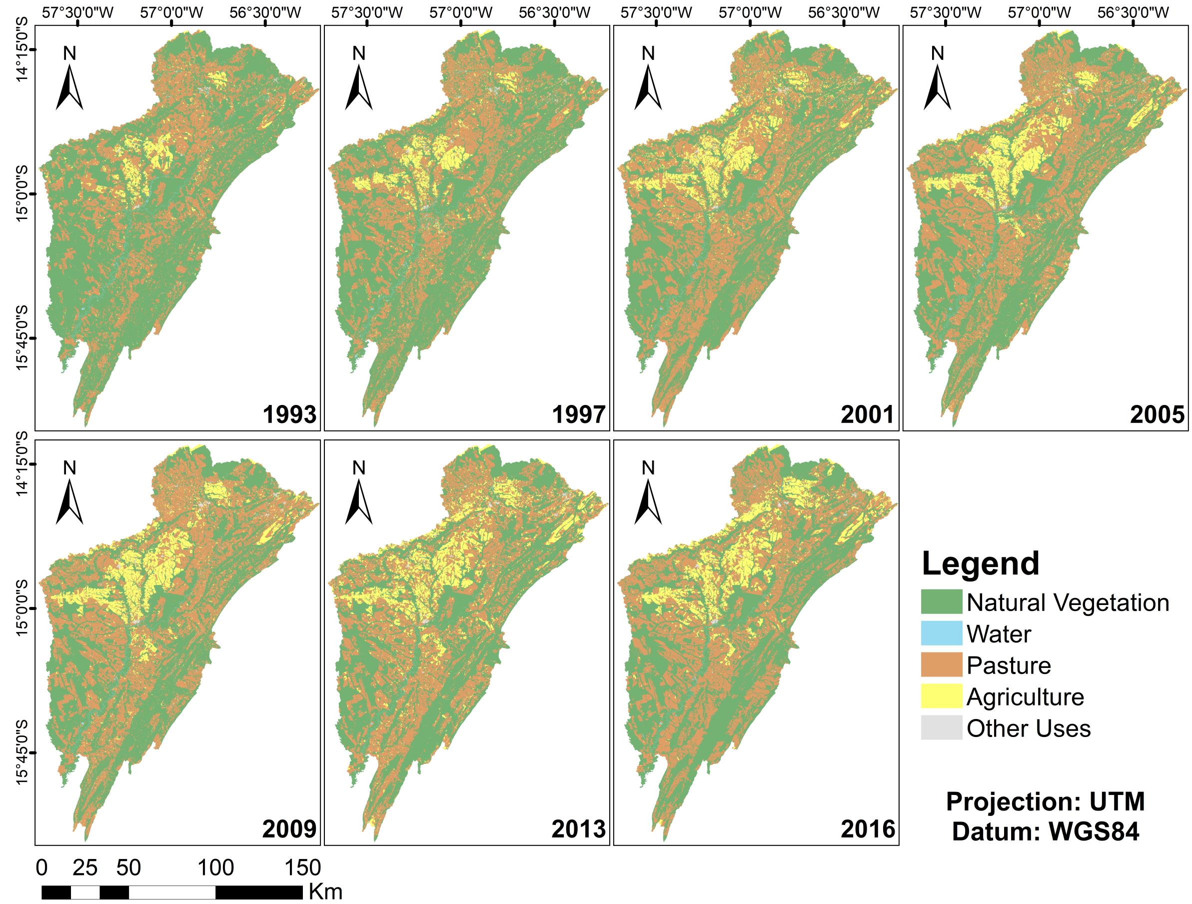

Figure 3: Distribution of thematic Land Use/Land Cover classes in the BHPJ.

generally has low-medium fertility (Ker, 2013). RP soil is mostly used for pasture activities on the tops and slopes of hills. Elevation was categorized by intervals of 100 m: 100–200m, 200–300m, 300–400m, 400–500m, and 500–600m.

3. Results and Discussion

3.1. Analysis of BHPJ data

Figure 3 provides an overview of the LULC classes that were present in the BHPJ from 1993 to 2016. The intensification of agricultural LULC and the decrease in the natural vegetation area can be observed.

Figure 4 hands an overview of the LULC changes in the BHPJ from 1993 to 2016 in terms of the average polygon area and the observed number of polygons. In particular, Figure 4 indicates that there has been a decreasing trend in the average area of natural vegetation polygons over the years. The decline is prominent in the first years; the rate was lower from 2005 to 2009 (also highlighted by Neto et al. (2009)), and an increase is seen in 2016. While the opposite has occurred with land used for pasture, agriculture (also reported in the temporal analysis by Ribeiro et al. (2016)) and other LULC use classes.

Therefore, it can be noted that the natural vegetation regions are disappearing and/or contracting and changing to pasture, agriculture, and other uses. According to Ribeiro et al. (2005), over the centuries, forests have been suppressed to allow the practice of economic activities such as agriculture, livestock rearing, and mining. Also, Casarin (2007) reported that forests, wetlands, and water sources were transformed into pasture in the Paraguay/Diamantino Basin, Mato Grosso. In particular, the LULC changes from agriculture to pasture can be due to the ever lower yields of various agricultural crops (Kosmas et al., 2000).

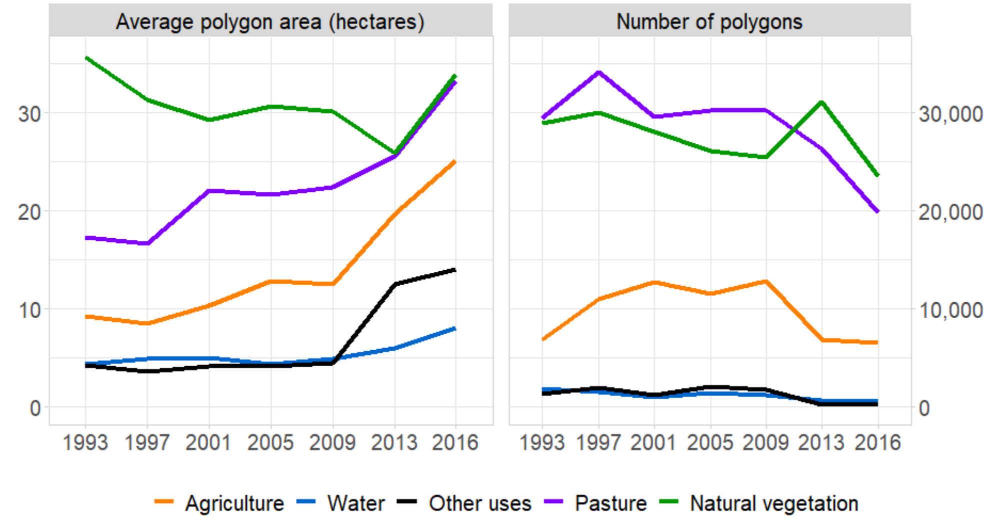

Figure 4: Evolution of the average polygon area and the number of polygons.

To understand the fragmentation caused by LULC change, a deep analysis of the number of polygons over time for each LULC class is relevant. Due to the LULC characteristics of the BHPJ, the number of polygons representing the LULC classes varied by orders of magnitude (right panel of Figure 4). For example, the number of natural vegetation polygons ranged from 23,514 to 31,089, while the number of water polygons was 565 to 1,947. This reflects the results for the large green areas and the rare water resources presented in Figure 3. Figure 5 shows that, for regions of natural vegetation larger than 0.5 hectares, the number of polygons sharply decreased. This may be due to conversion of the area into pasture and agriculture or destruction or degradation of habitat by wild fire, water pollution, unsustainable tourism, or the introduction of invasive exotic species (Alho and Sabino, 2011). Moreover, the dryness observed over time was confirmed by the decreasing number of polygons for all ranges of water areas. For the natural vegetation and pasture LULC classes, the number of polygons, in general, decreased across the range of area, independently of the year, which implies that these areas are more fragmented than the remaining areas. Furthermore, for the agriculture and pasture classes, the number of polygons of smaller areas decreased, but the number of polygons of larger areas increased and remained. The expansion of larger agricultural areas and the reduction of natural vegetation areas were also observed in the data presented in Figure 3. In summary, Figure 5 suggests that there were relevant changes in LULC classes from 2009 to 2016, mainly in agriculture regions.

Spatial LULC data tend to be dependent (Overmars et al., 2003), once most biophysical processes exhibit spatial autocorrelation (Munroe et al., 2001). That is, random variables have values over distance that are more or less similar than expected for randomly associated pairs of observations. This phenomenon is known as spatial autocorrelation, and it was studied using the statistical test described in Section 2.3.1.

For all data sets corresponding to each year and each LULC class, the observed p-values were less than 0.05, so it is reasonable to assume the presence of spatial autocorrelation. Furthermore, all observed values were higher than the corresponding expected values, which is an indicator of clustering (positive spatial autocorrelation). Thus, the closest regions were more similar than the distant ones, reflecting the interaction between sites, since most changes are consequences of anthropogenic activities and these also exhibit neighborhood effects (Munroe et al., 2001).

Since the number of joins allows assessment of the degree of clustering or dispersion (Section 2.3.1), the analysis of the percentage of BB joins over time by LULC class may be very informative (Figure 6). The results presented in Figure 6 enable visualization of a decreasing tendency of the percentage of BB joins for the pasture and natural vegetation areas, and an increasing trend for the agriculture areas. Despite the observed values for the agriculture and natural vegetation areas in 2013, the pasture and natural vegetation areas were sparser and the agriculture areas more clustered over time. This pattern in

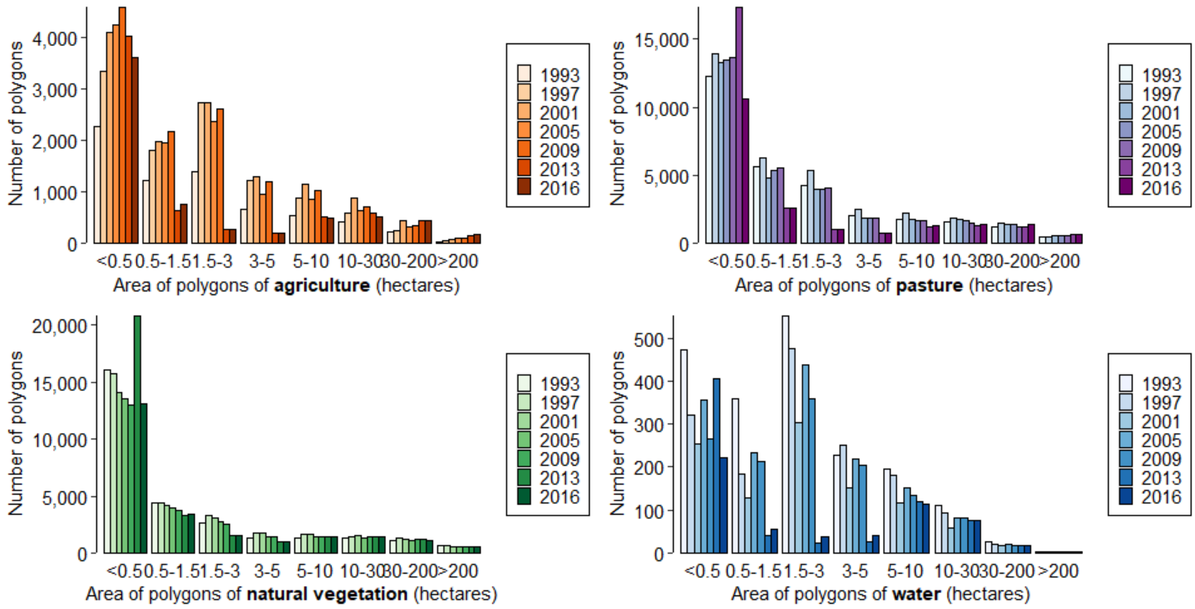

Figure 5: Comparison of polygon areas of LULC classes among different years.

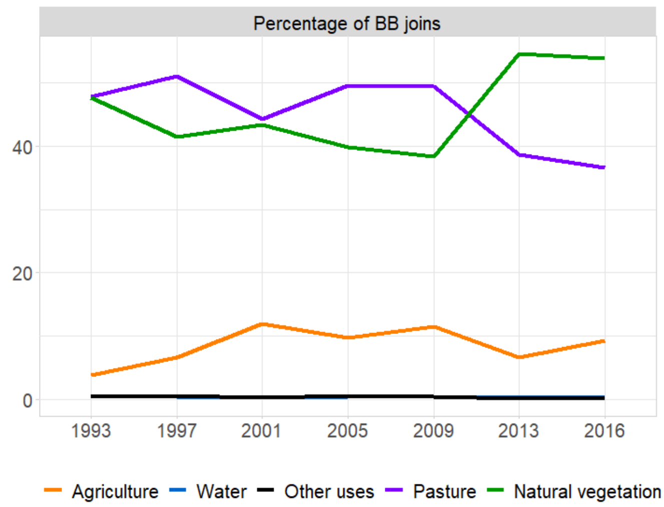

Figure 6: Percentage of the number of BB joins by LULC class.

agricultural areas can be justified by the importance of this activity for the Mato Grosso state. In fact, farming and raising cattle were defined as the main economic activities of this state, representing almost 30% of the state's gross domestic product, and agriculture accounted for 23% of this percentage (Mato Grosso (Estado). Secretaria de Estado de Planejamento e Coordenação Geral – Seplan, 2012). In short, the data verified that there was an increase in agricultural regions at the expense of natural vegetation and pasture zones, which contracted or disappeared. Furthermore, the increase in BB joins for the natural vegetation LULC class in 2013 can be justified by the increase in the respective area.

3.2. Analysis of Bugres river basin data

As alluded to in Section 2.3, this spatio-temporal analysis was fostered by the growth of agricultural areas over time. Table 1 shows the number of regions and the corresponding total areas over time, and Figure 7 presents the evolution of the agricultural regions' area in the BHRB.

Table 1: Observed number of regions and total area over time.

Year	1993	1997	2001	2005	2009	2013	2016
Number of regions	427	841	1149	653	767	444	308
Total area (hectares)	32,880.98	40,137.70	61,458.97	73,416.89	74,566.48	71,395.65	67,762.06

Table 1 shows that the number of regions and the corresponding total area for agriculture were not correlated (for instance, in 1993 and 2013, almost the same number of polygons was observed, but the total areas were very different). However, there was a pattern of growth in the total agriculture area until 2009, which is an indicator of expansion according to Pessoa et al. (2014). The observed decreases in 2013 and 2016 show a change in the BHRB agricultural area. Therefore, the results indicate that changes were occurring in space and time. In particular, Figure 7 shows the changes that occurred in the sizes of regions, which mainly happened in the south, where some regions were increasing and others decreasing without a well-defined pattern. The northern area comprises smaller areas, and it seemed to present a more discrete evolution of sizes over the years. Overall, these changes may indicate the expansion and contraction of agricultural regions. These results indicate the importance and relevance of spatio-temporal moving polygon analysis.

The acquired data included seven periods; therefore, six change intervals were included in the analysis of topological events; these were labeled 1–6 in ascending order. Analysis was restricted to a level 2 change indicator, once at least 98% of agricultural area remained, generated, disappeared, contracted, or expanded, which revealed that displacement, convergence, divergence, concentration, and fragmentation were rare in agricultural regions' changes over time (see Table A.2 from Appendix A). Figure 8 provides an overview of this indicator in the BHRB over the six change intervals. Most regions remained stable over time, while the disappearance and the appearance of regions were rare when compared with the expansion and contraction events.

Even though the expansion event was significant in the first change interval, there was a decreasing trend in this event until 2009, and an increase in contraction events. Hence, this resulted in a balance between these events in the following years. Another important inference based on the level 2 changes indicator was that the regions that appeared or expanded in a certain time frame ended up disappearing or contracting, indicating a greater change in the BHRB agricultural regions.

Next, the geographical area, soil type, and elevation were investigated due to the noticeable differences in these variables (Figure 7). Spatial representation of these variables is presented in Figure 9. Most of the BHRB agricultural areas are at low elevation (100–300m) and use RL

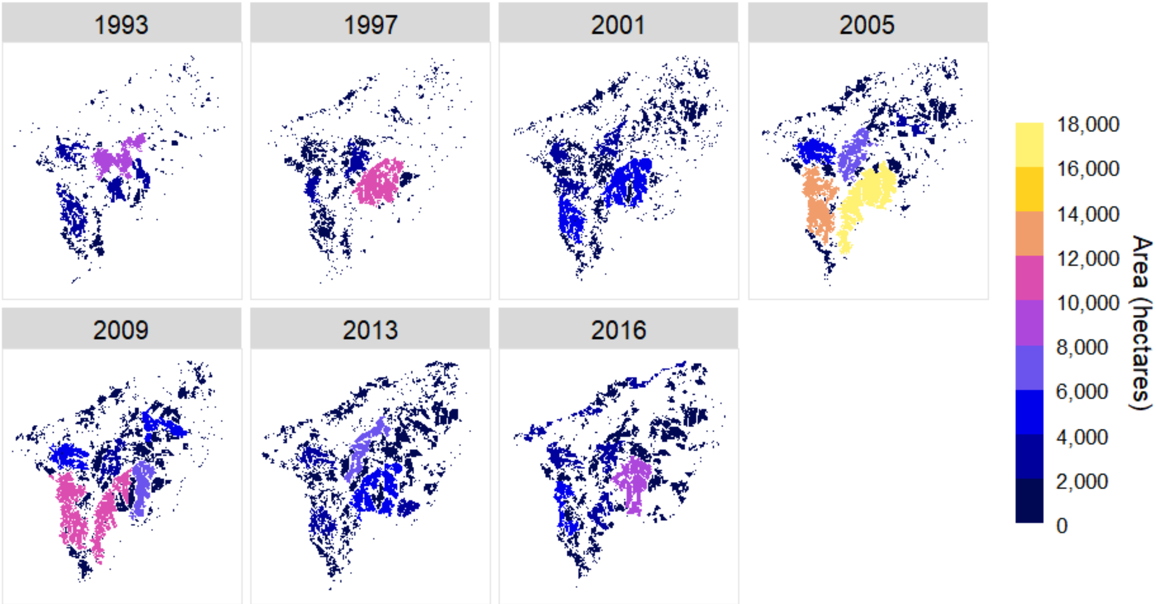

Figure 7: Evolution of the area of agricultural regions.

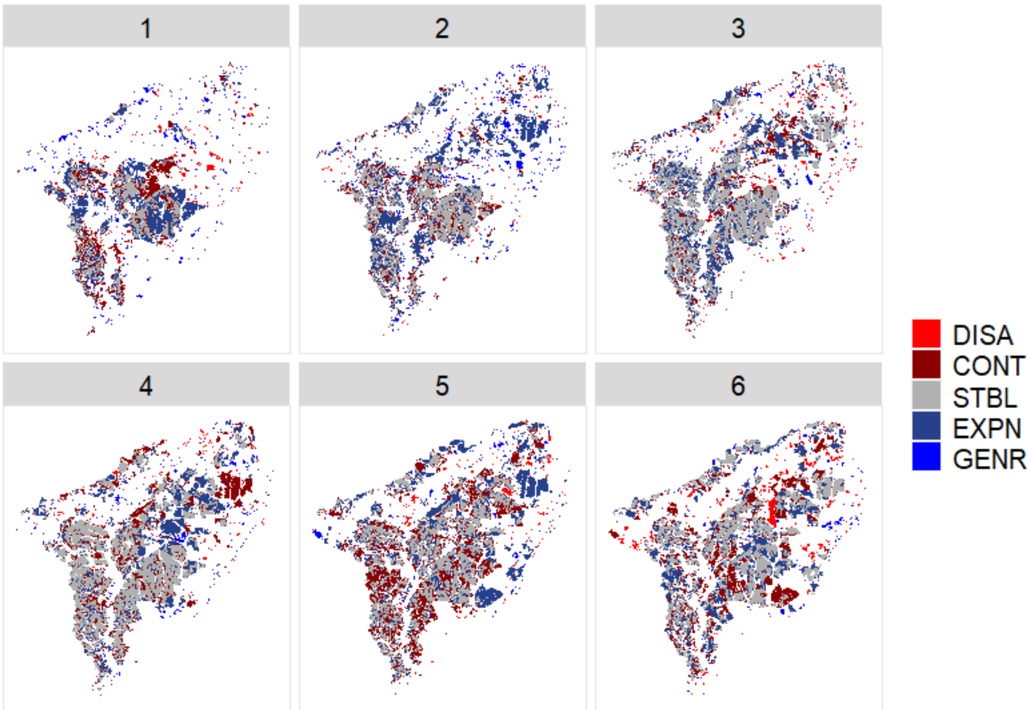

Figure 8: Level 2 topological events: GENR (generation), EXPN (expansion), STBL (stable), CONT (contraction) and DISA (disappearance).

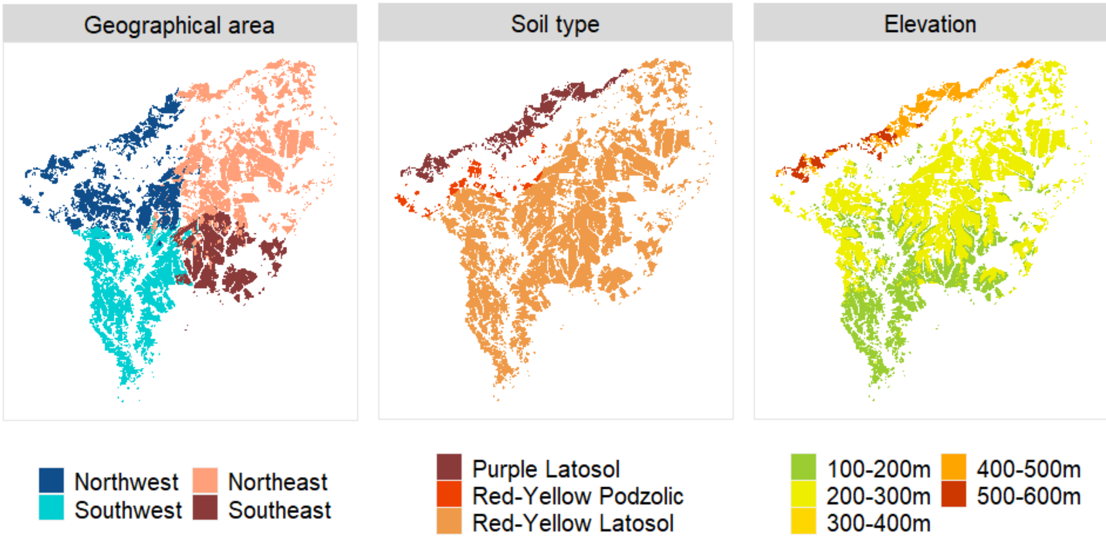

Figure 9: Geographical area, soil type and elevation maps.

soil. Higher areas (400–600m) seem to be associated with PL soil (see Figure 9). Additionally, the elevation increases from south to north of the basin.

Analysis of Table A.2 in Appendix A indicated that there was a pattern in contraction and expansion events mainly in the western and southeastern areas. More specifically, there was more area expanding than contracting until 2005, and then the pattern changed. In the northeast, since 2005, the stable agricultural area has been larger than the contracting area, with variations in the expansion area rate over time. Therefore, it may suggest that since 2005 there has been a stabilization of agricultural regions, which indicates a slowdown in its expansion. This fact is congruent with the observed stabilization of intensive agricultural areas since 2006 in BAP by Coutinho et al. (2016).

Similarly,Table A.3 in Appendix A shows the changes in areas by soil type. The PL soil type corresponded to the highest expansion indexes since 2001, the RL soil type corresponded to the highest stabilization percentage until 2013, and the RP soil type corresponded to the highest generation rates since 2001, despite its decreasing trend and showing the highest disappearing percentage over time. Also, worthy of note is the observation that the fertility of PL soil seems to be higher than that of the other latosols (Ker, 2013), which likely explains the larger stabilization observed in this soil type.

Furthermore, different change patterns were observed according to the elevation (see Table A.4 in Appendix A). For lower lands, there was more contraction than expansion, in terms of the change area percentage since 2005. In contrast, areas at 200–300m, 400–500m, and 500–600m recorded more expansion events than contraction events, except during change intervals 6, 4 and 5, respectively. Despite the contraction area being larger than the expansion area for elevations of 200–300m and 500–600m in the 6 and 5 change intervals, respectively, the difference between the agricultural area expansion and contraction was very small. Lower agricultural lands (100–300m) were more stable than areas at 300–600m; this was also observed by Opršal et al. (2016). The generation event was the most observed event at higher elevations during the first interval change, and then expansion/stabilization events dominated.

Another index of change, described in Section 2.3.2, was the distance between moving regions. Since the distance index is given by the distance between two regions from different years, it allows analysis of the evolution of region movement. In particular, for contracting regions, an increase in distance may indicate that the area of the region has decreased and its shape and location have changed. The four geographical areas (Figure 10a), the three soil types (Figure 10b), and the various elevation classes (Figure 10c) may also display different patterns in terms of the distance of contracting and expanding regions, so the average of the distance by time interval was computed.

We may conclude that agricultural regions have been contracting and expanding at increasingly distant places in the north and southwestern areas, which also reflects an increasingly drastic change. Furthermore, Figure 10a suggests that changes in the southwest occur at a higher level than in the remaining areas in terms of distance. While in the southeastern area, the average distance from the events of contraction has been constant regardless of the class of change, despite the larger variation in terms of distance. This allows us to conclude that there has been more change in contracting areas than in expanding areas over time in the southeastern area.

The average of change distance for PL soil exhibited an exponential behavior, which was also observed for higher elevations ($\geq$300m). In fact, higher elevations are associated with the PL soil type, as confirmed by Figure 9. Nevertheless, the contraction occurred at more distant places than the expansion regarding areas with elevation between 400m and 600m, while the average distance of expanding and contracting moving areas were similar over time at 300–400m. Therefore, in agricultural regions at higher elevations, there were more significant contracting changes than expanding ones in terms of moving distance. Similarly, an increase in the contracting distance over time for RL soil areas was confirmed. In the RP soil type, the moving distance of expansion and contraction decreased until 2009 and 2013, respectively, and then the change index started to increase.

It was noted that the contracting distance was larger than the expanding distance for the last two intervals of change. Comparing the regions at 100–200m and 200–300m, similar patterns of expanding and contraction average distance were found, although the values were lower for the second elevation class. Thus, regions at 100–200m exhibited greater indexes of change than the remaining regions until 2013 in terms of the moving distance, possibly due to the propensity for agricultural practice in these areas, as stated by Warra et al. (2015) and Opršal et al. (2016). However, higher areas presented greater average distance in 2016 for both contraction and expansion events, likely explained by the farmers' necessity to expand agricultural regions to higher elevations (Warra et al., 2015).

The changes in moving regions may also be explained in terms of their direction, as discussed in Section 2.3.2 (see Figure 11). Figure 11a shows distinct patterns of direction change for the different soil types and Figure 11b for the elevation classes. Until 2009, larger areas of RL soil were expanding to the south, while contraction was occurring in all directions from 2009. In the PL soil, there was less contraction in the northwest, a decreasing trend of expansion to the southeast was verified, and the expansion event was higher in the southwest over the last three change intervals.

Furthermore, most of the areas at an elevation of 100–200m were found to be moving to the south despite the observed decrease in corresponding area in the last year, while expansion mostly occurred to the north over time, at an elevation of 200–300m. At an elevation of 400–500m, there was a decreasing trend of contraction in the northwest, presenting a contraction rate in this direction lower than 4% in the last year. Regarding areas at 500–600m, most changes occurred to the southwest. In particular, the contraction rate increased over time, although most expanding regions also moved in this direction. The expansion rate was higher than the contraction rate in only the second and third change intervals, highlighting agricultural

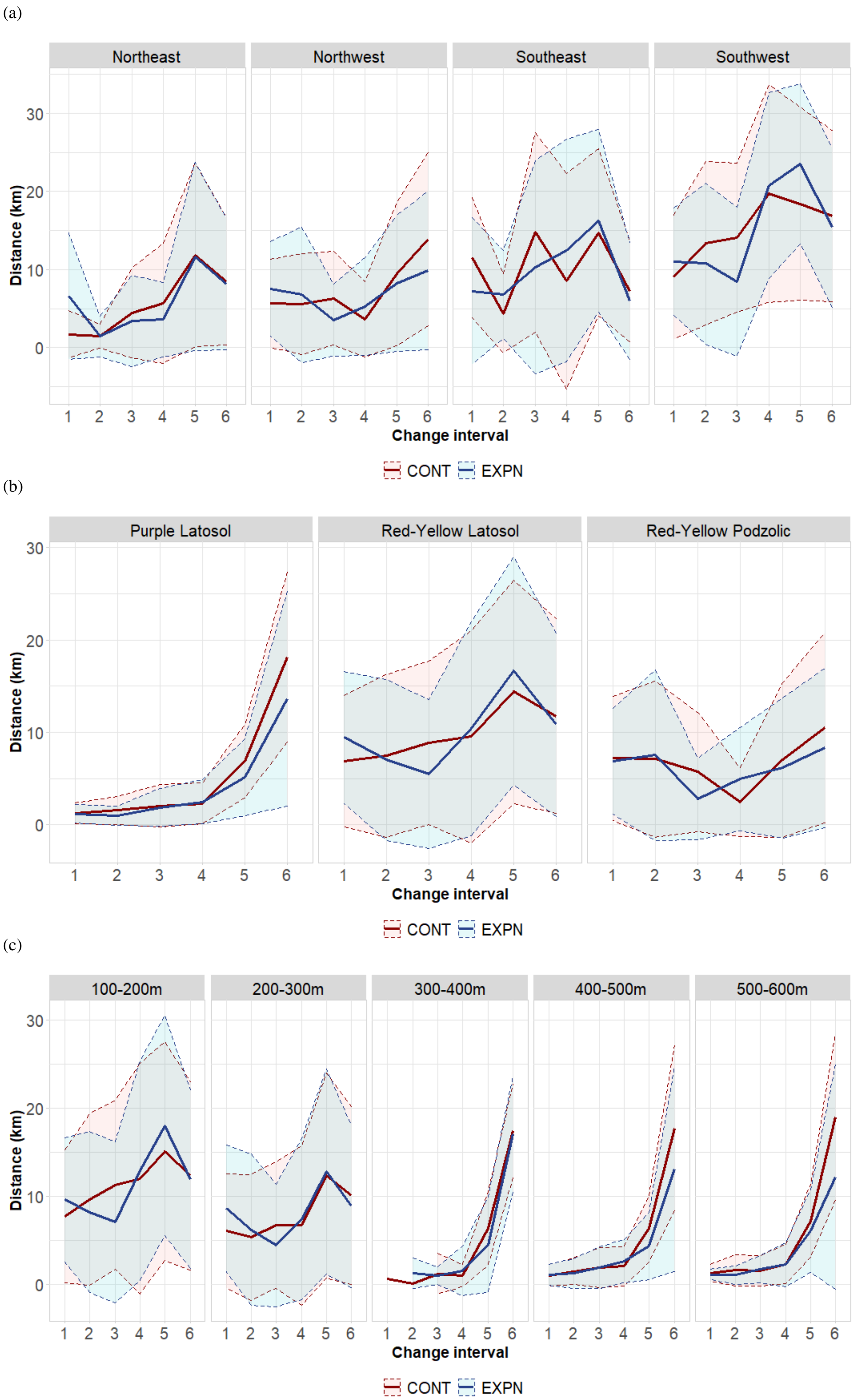

Figure 10: Average and standard deviations for Hausdorff distance over change interval and topological event (CONT and EXPN) by geographical area (a), soil type (b) and elevation class (c).

(a)

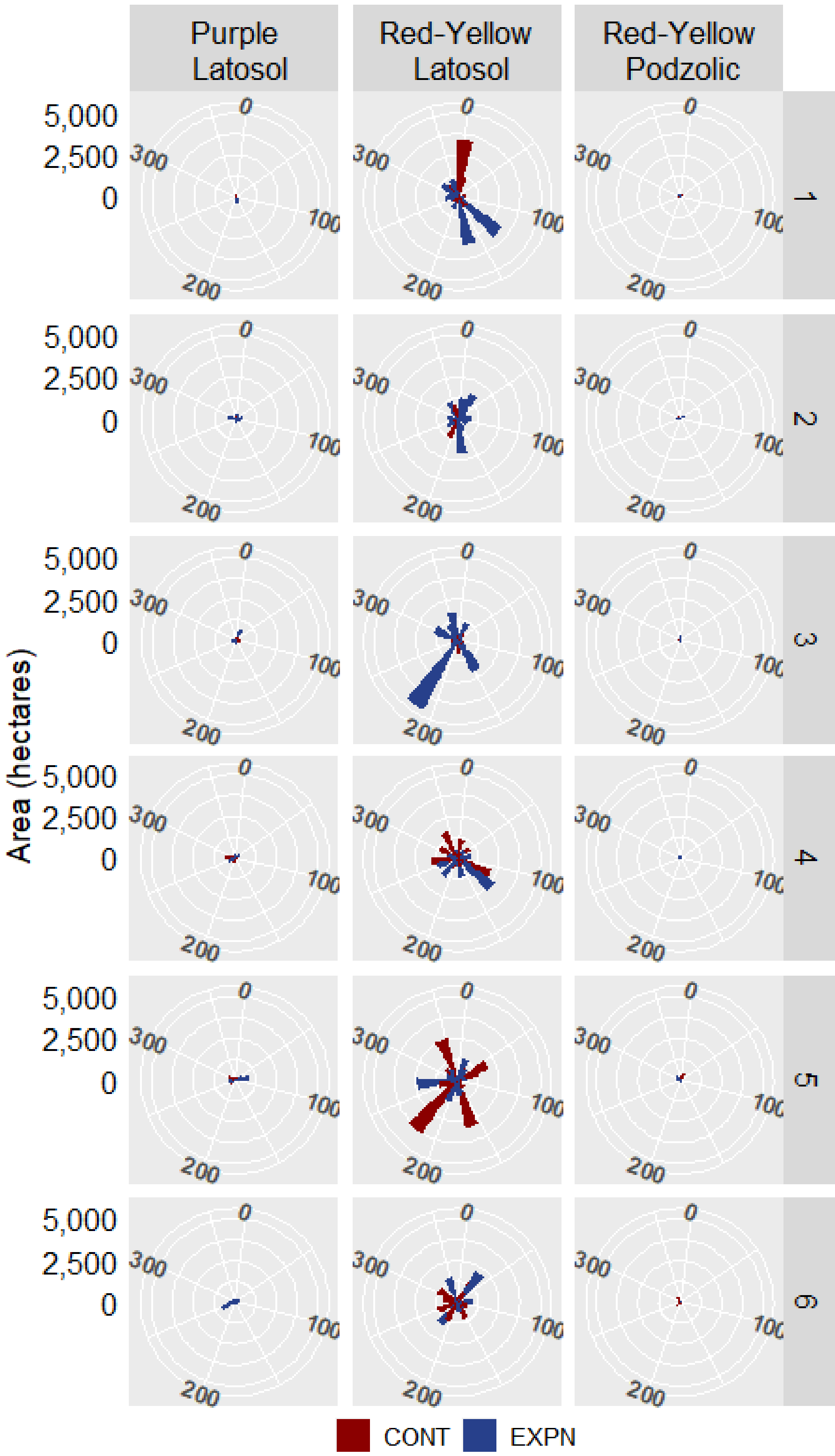
Purple Latosol
Red-Yellow Latosol
Red-Yellow Podzolic
Area (hectares)
5,000
2,500
0
0
100
200
300
1
2
3
4
5
6
CONT
EXPN

(b)

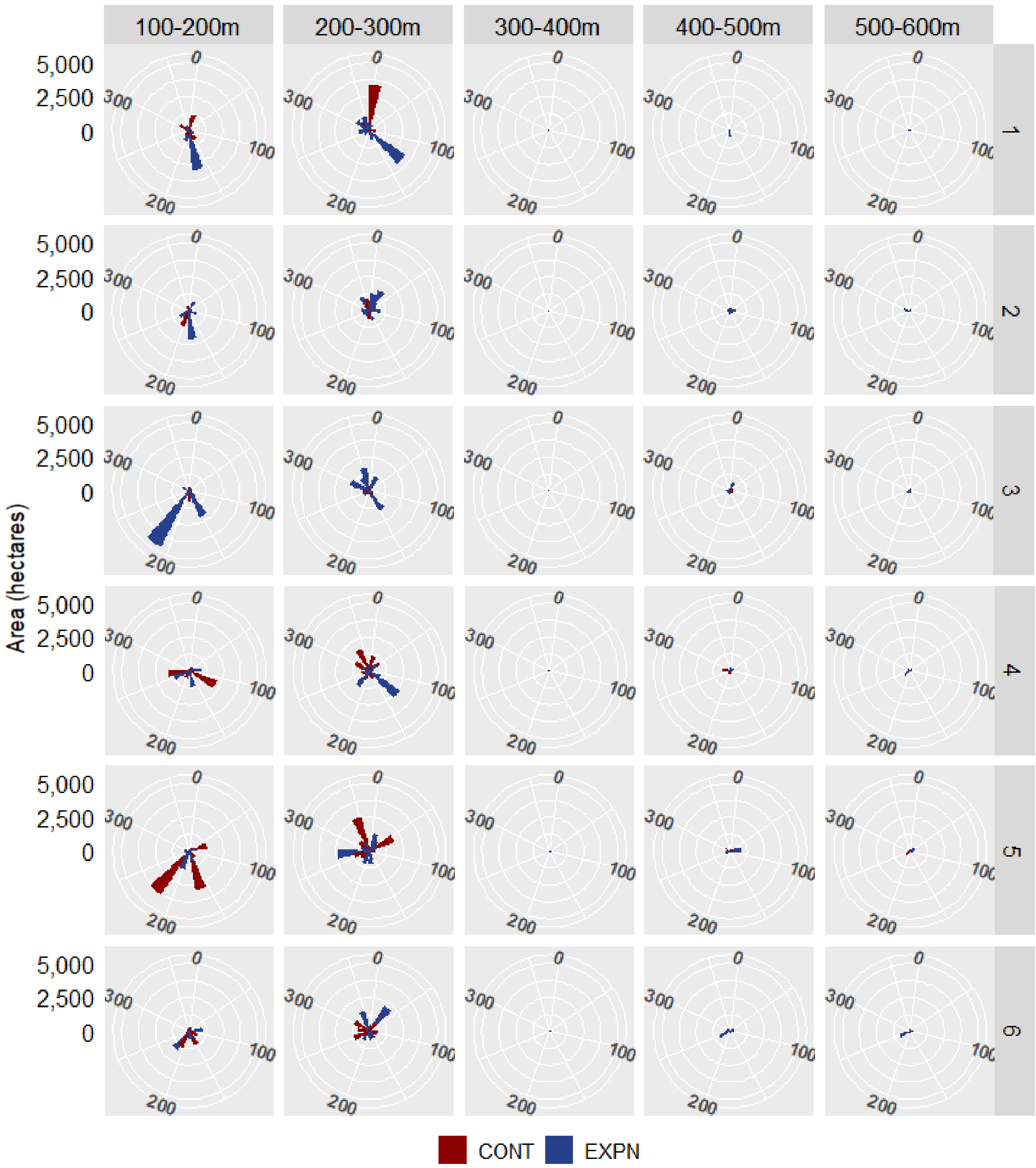

Figure 11: Directional changes over change interval and topological event (CONT and EXPN) by soil type (a) and elevation class (b).

deintensification. It is also noteworthy that the events of contraction and expansion did not always occur in opposite directions.

4. Conclusion

A spatio-temporal analysis of LULC changes was conducted. The results were used to determine the general changes in the BHPJ and to analyze the specific changes in agricultural areas in the BHRB. Data for the analysis were obtained from multi-year satellite imagery, processed using ArcGIS software, and subjected to statistical analysis in the R environment.

The statistical analysis incorporated exploratory methods and a study of spatial dependency. We concluded that natural vegetation is disappearing and/or contracting and changing to pasture, agriculture and land for other uses, reflecting economic practices and other human activities.

The spatial dependency study pointed to a significant interaction between the locations, indicating that the closest regions are similar. In particular, the agricultural area has been increasingly concentrated, since this similarity is growing. The spatio-temporal analysis of moving agricultural areas consisted of the categorization of polygon changes and their combination with metrics such as area, number of patches, distance, and direction of change. This analysis revealed an expansion of the agricultural area but also its stabilization since 2005. However, the pattern of change was different across the study area. Thus, agricultural regions are contracting and expanding at increasingly distant places in the BHRB. In fact, greater changes were observed between 1993 and 2016.

This study demonstrated that the combination of remote sensing, GIS, and spatio-temporal analysis offers relevant results for analyzing LULC change. In fact, it can add value to studies related to the planning and management of land and biodiversity conservation.

Nevertheless, this analysis has strengths and limitations. The strengths are the easy interpretation of the outputs, the simplicity of the metrics used, the deep study of changes with the incorporation of distance and direction metrics, and the friendly environment used to perform it (R software). However, the purpose of this study was to assess the dynamics of LULC changes and project them into the future, and not to predict the LULC. Another limitation of this work is the time-consuming nature of the categorization of polygon changes for big data.

Therefore, one direction for future study is to develop a predictive method that takes into account the restrictions and characteristics of LULC data and introduces environmental/biological and economic variables to the polygon data format.

Appendix A. Evolution of the percentage of the topological events area by explanatory factors

Table A.2: Evolution of the percentage of the topological events area by geographical area

Geographical area	LEV3	Change interval					
		1	2	3	4	5	6
Northeast	CONC	0.02	0.01	0.04	0.00	0.00	0.00
	CONT	31.81	9.15	22.70	25.70	22.81	22.90
	CONV	0.00	0.06	0.10	0.01	0.00	0.00
	DISA	10.58	4.23	7.99	3.76	4.71	10.20
	DISP1	1.68	0.20	0.15	0.01	0.00	0.00
	DISP2	0.04	0.15	0.37	0.01	0.00	0.00
	DIVR	0.01	0.06	0.49	0.05	0.06	0.00
	EXPN	28.94	56.70	30.32	34.02	39.34	25.17
	FRAG	0.00	0.18	0.00	0.01	0.00	0.00
	GENR	12.48	23.59	4.45	5.36	3.22	3.71
	STBL	14.43	5.67	33.39	31.07	29.86	38.01
Northwest	CONC	0.00	0.00	0.07	0.00	0.00	0.00
	CONT	19.88	20.71	12.60	22.89	26.76	22.02
	CONV	0.00	0.00	0.00	0.15	0.03	0.00
	DISA	2.32	2.01	2.79	2.15	2.91	4.95
	DISP1	0.00	0.08	0.01	0.06	0.00	0.00
	DISP2	0.00	0.06	0.01	0.17	0.00	0.00
	DIVR	0.01	0.03	0.03	0.04	0.10	0.00
	EXPN	35.01	34.13	30.77	19.33	22.39	21.53
	FRAG	0.00	0.14	0.00	0.03	0.00	0.00
	GENR	9.56	3.61	2.65	2.40	2.91	1.92
	STBL	33.22	39.24	51.07	52.78	44.91	49.58
Southeast	CONC	0.00	0.00	0.00	0.00	0.07	0.00
	CONT	9.92	7.53	3.63	17.98	25.54	20.13
	CONV	0.00	0.37	0.00	0.00	0.00	0.00
	DISA	2.24	2.21	3.83	1.04	1.55	0.81
	DISP1	0.00	0.00	0.00	0.00	0.00	0.00
	DISP2	0.00	0.00	0.00	0.00	0.00	0.00
	DIVR	0.00	0.00	0.00	0.00	0.00	0.00
	EXPN	52.69	10.83	17.66	13.14	26.64	17.86
	FRAG	0.00	0.00	0.00	0.00	0.00	0.00
	GENR	5.53	3.58	1.60	2.51	1.21	1.60
	STBL	29.61	75.48	73.29	65.32	44.99	59.60
Southwest	CONC	0.00	0.02	0.01	0.00	0.13	0.00
	CONT	28.65	18.92	11.64	15.80	36.60	29.94
	CONV	0.04	0.00	0.05	0.00	0.04	0.00
	DISA	2.18	1.02	1.08	0.38	0.82	1.64
	DISP1	0.00	0.01	0.02	0.01	0.00	0.00
	DISP2	0.00	0.02	0.01	0.01	0.00	0.00
	DIVR	0.03	0.12	0.00	0.03	0.00	0.00
	EXPN	30.16	38.80	30.47	15.69	14.52	28.38
	FRAG	0.03	0.01	0.01	0.03	0.00	0.00
	GENR	4.65	2.44	0.47	0.76	0.46	0.94
	STBL	34.27	38.64	56.24	67.29	47.44	39.11

Table A.3: Evolution of the percentage of the topological events area by soil type

Soil type	LEV2	Change interval					
		1	2	3	4	5	6
Purple Latosol	CONT	6.39	13.49	20.66	28.28	24.48	13.11
	DISA	8.64	2.85	4.23	5.56	1.65	2.77
	EXPN	25.44	48.71	32.71	29.12	40.14	30.99
	GENR	49.02	8.40	6.48	2.21	2.56	3.05
	STBL	10.50	26.55	35.92	34.83	31.16	50.09
Red-Yellow Latosol	CONT	25.01	15.43	13.71	20.35	28.81	24.54
	DISA	4.55	2.05	3.71	1.49	2.34	5.02
	EXPN	35.22	37.00	28.81	21.26	24.93	23.81
	GENR	5.87	7.98	1.93	2.61	1.61	2.07
	STBL	29.35	37.53	51.85	54.28	42.31	44.56
Red-Yellow Podzolic	CONT	29.61	18.58	14.42	20.92	19.17	45.02
	DISA	9.54	10.85	11.27	8.81	15.10	20.14
	EXPN	21.93	37.42	28.28	23.35	32.04	9.69
	GENR	22.88	13.30	12.76	13.75	12.58	4.66
	STBL	16.04	19.85	33.27	33.17	21.11	20.49

Table A.4: Evolution of percentage of the topological events area by elevation categories

Elevation	LEV2	Change interval					
		1	2	3	4	5	6
100-200m	CONT	27.57	17.72	11.12	19.47	34.45	29.72
	DISA	3.99	2.71	3.12	1.01	2.52	3.69
	EXPN	33.83	34.73	31.09	17.61	20.43	24.86
	GENR	6.41	5.90	1.68	2.88	1.59	2.40
	STBL	28.19	38.94	52.99	59.04	41.01	39.33
200-300m	CONT	23.29	14.17	15.32	21.10	24.89	22.84
	DISA	5.24	2.09	4.23	2.03	2.94	6.63
	EXPN	35.68	38.74	27.44	23.48	27.76	22.44
	GENR	6.20	9.12	2.54	3.00	2.35	2.04
	STBL	29.59	35.88	50.48	50.39	42.06	46.04
300-400m	CONT	39.09	2.21	14.82	12.44	29.40	43.35
	DISA	44.96	9.02	22.53	22.39	15.72	8.36
	EXPN	0.00	8.60	45.51	45.37	28.36	25.46
	GENR	15.95	78.67	10.00	12.19	3.00	5.09
	STBL	0.00	1.51	7.13	7.61	23.52	17.74
400-500m	CONT	7.23	11.06	20.67	31.25	21.79	11.79
	DISA	8.11	2.42	6.08	7.76	2.46	1.84
	EXPN	27.95	46.48	30.21	23.74	47.28	30.11
	GENR	44.18	10.70	6.66	2.69	3.22	2.85
	STBL	12.53	29.34	36.38	34.56	25.25	53.41
500-600m	CONT	3.40	18.37	22.55	19.07	28.73	17.11
	DISA	7.40	3.42	4.69	2.83	2.16	4.29
	EXPN	15.53	47.57	32.62	41.78	28.73	31.82
	GENR	69.92	13.46	8.09	2.36	1.00	2.91
	STBL	3.74	17.17	32.05	33.96	39.38	43.86

References

Alho, C., Sabino, J., 2011. Conservation agenda for the Pantanal's biodiversity. Brazilian journal of biology 71, 327–335. doi:10.1590/S1519-69842011000200012.

Bivand, R., 2020. spdep: Spatial Dependence: Weighting Schemes, Statistics. URL: https://github.com/r-spatial/spdep/.

Brasil, 1982. Decreto Nº 87.222, de 31 de Maio 1982. URL: http://www.planalto.gov.br/ccivil_03/Atos/decretos/1982/D87222.html. (Accessed on 6 January 2019).

Brasil. Ministério do Meio Ambiente e Instituto Brasileiro de Geografia – IBGE, 2004. Mapa de Biomas do Brasil - 1:5000000. URL: https://www.ibge.gov.br/geociencias/informacoes-ambientais/15842-biomas.html?edicao=16060&t=sobre. (Accessed on 20 July 2018).

Casarin, R., 2007. Caracterização dos principais vetores de degradação ambiental da bacia hidrográfica Paraguai/Diamantino. Ph.D. thesis. UFRJ/GEOCIÊCIAS. Rio de Janeiro.

Cliff, A.D., Ord, J.K., 1981. Spatial processes. Pion Limited, London.

Câmara, G., Souza, R., Freitas, U., Garrido, J., 1996. Spring: integrating remote sensing and GIS by object-oriented data modelling. Computers & Graphics 20, 395–403. doi:10.1016/0097-8493(96)00008-8.

Coutinho, A.C., Bishop, C., Esquerdo, J.C.D.M., Kastens, J.H., Brown, J.C., 2016. Dinâmica da agricultura na Bacia do Alto Paraguai, in: Anais 6º Simpósio de Geotecnologias no Pantanal, Embrapa Informática Agropecuária/INPE, Cuiabá. pp. 623 –632.

ESRI, R., 2011. ArcGIS desktop: release 10. Environmental Systems Research Institute, CA .

Fenner, W., Moreira, P.S.P., Ferreira, F.d.S., Dallacort, R., Queiroz, T.M., Bento, T.S., 2014. Análise do balanço hídrico mensal para regiões de transição de Cerrado-Floresta e Pantanal, Estado de Mato Grosso. Revista Acta Iguazu 3, 72–85.

French, K., Li, X., 2010. Feature-based cartographic modelling. International Journal of Geographical Information Science 24, 141–164. doi:10.1080/13658810802492462.

Galvanin, E., Menezes, R., Pereira, M.H.X., Neves, S.M., 2019. Mixed-effects modeling for analyzing land use change in the Brazilian Pantanal subregion of Cáceres. Remote Sensing Applications: Society and Environment 13, 408–414. doi:10.1016/j.rsase.2018.12.008.

Gao, J., O'Neill, B., 2019. Data-driven spatial modeling of long-term urban land development potential for global environmental change impact assessment: The SELECT model. Environmental Modelling & Software 119, 458–471. doi:10.1016/j.envsoft.2019.06.015.

Garcia-Soidan, P., Menezes, R., 2012. Estimation of the spatial distribution through the kernel indicator variogram. Environmetrics 23, 535–548. doi:10.1002/env.2151.

Getis, A., 2010. Spatial Autocorrelation, in: Fisher, M.M., Getis, A. (Eds.), Handbook of Applied Spatial Analysis: Software tools, methods and applications. Springer, Berlin, Heidelberg, pp. 255–278. doi:10.1007/978-3-642-03647-7_14.

IBGE, 2012. Manual Técnico da Vegetação Brasileira. 3 ed. Rio de Janeiro.

ISA, I.S., 2018. Serviço de Proteção aos Índios (SPI). URL: https://pib.socioambiental.org/pt/Servi%C3%A7o_de_Prote%C3%A7%C3%A3o_aos_%C3%8Dndios_(SPI). (Accessed on 22 September 2020).

Jacobson, A., Dhanota, J., Godfrey, J., Jacobson, H., Rossman, Z., Stanish, A., Walker, H., Riggio, J., 2015. A novel approach to mapping land conversion using Google Earth with an application to East Africa. Environmental Modelling & Software 72, 1 – 9. URL: http://www.sciencedirect.com/science/article/pii/S1364815215001747, doi:10.1016/j.envsoft.2015.06.011.

Ker, J.C., 2013. Latossolos do Brasil: Uma revisão. Geonomos 5, 17–40. doi:10.18285/geonomos.v5i1.187.

Kosmas, C., Gerontidis, S., Marathianou, M., 2000. The effect of land use change on soils and vegetation over various lithological formations on Lesvos (Greece). CATENA 40, 51–68. doi:10.1016/S0341-8162(99)00064-8.

Long, J., Robertson, C., 2018. stampr: Spatial Temporal Analysis of Moving Polygons. URL: https://CRAN.R-project.org/package=stampr.

Lu, D., Li, G., Moran, E., Hetrick, S., 2013. Spatiotemporal analysis of land use and land cover change in the Brazilian Amazon. International journal of remote sensing 34, 5953–5978. doi:10.1080/01431161.2013.802825.

Lu, D., Mausel, P., Brondízio, E., Moran, E., 2004. Change detection techniques. International Journal of Remote Sensing 25, 2365–2401. URL: https://doi.org/10.1080/0143116031000139863, doi:10.1080/0143116031000139863, arXiv:https://doi.org/10.1080/0143116031000139863.

Machado, R., Bayot, R., Godinho, S., Pirnat, J., Santos, P., de Sousa-Neves, N., 2020. LDTtool: A toolbox to assess lanscape dynamics. Environmental Modelling & Software 133.

Mato Grosso (Estado). Secretaria de Estado de Planejamento e Coordenação Geral – Seplan, 2012. Plano de Longo Prazo de Mato Grosso : macro-objetivos, metas globais, eixos estratégicos e linhas estrutantes. MT : Central de Texto, Cuiabá. ISBN 978-85-8060-005-6.

Menezes, R., Piairo, H., García-Soidán, P., Sousa, I., 2016. Spatial–temporal modellization of the no2 concentration data through geostatistical tools. Journal of Statistical Methods & Applications 25, 107–124. doi:10.1007/s10260-015-0346-3.

Mizutani, C., Murayama, Y., 2011. Analytical framework for polygon-based land use change. SIGSPATIAL Special 3, 15–20. doi:10.1145/2078296.2078300.

Monzilar, E., 2018. Território Umutina: vivências e sustentabilidade. Revista Tecnologia e Sociedade 14, 122–143. doi:10.3895/rts.v14n34.7265.

Morris, R., 2010. Anthropogenic impacts on tropical forest biodiversity: A network structure and ecosystem functioning perspective. Philosophical transactions of the Royal Society of London. Series B, Biological sciences 365, 3709–18. doi:10.1098/rstb.2010.0273.

Munroe, D.K., Southworth, J., Tucker, C.M., 2001. The Dynamics Of Land-Cover Change In Western Honduras: Spatial Autocorrelation And Temporal Variation. 2001 Annual meeting, August 5-8, Chicago, IL 20759. American Agricultural Economics Association (New Name 2008: Agricultural and Applied Economics Association). URL: https://ideas.repec.org/p/ags/aaea01/20759.html, doi:10.22004/ag.econ.20759.

Neto, E.R.S., Neves, R.J., da Silva Neves, S.M.A., 2009. Análise multitemporal do desmatamento na bacia hidrográfica do Paraguai/Jauquara – Mato Grosso, Brasil, in: 2º Simpósio de Geotecnologia no Pantanal, Embrapa Informática Agropecuária/INPE, Corumbá. pp. 1009–1017.

Opršal, Z., Kladivo, P., Machar, I., 2016. The role of selected biophysical factors in long-term land-use change of cultural landscape. Applied Ecology and Environmental Research 14, 23–40. doi:10.15666/aeer/1402_023040.

van Oudenhoven, A., Petz, K., Alkemade, R., Hein, L., Groot, R., 2012. Framework for systematic indicator selection to assess effects of land management on ecosystem services. Ecological Indicators 21, 110–122. doi:10.1016/j.ecolind.2012.01.012.

Overmars, K., Koning, G., Veldkamp, A., 2003. Spatial Autocorrelation in Multi-Scale Land Use Models. Ecological Modelling 164, 257–270. doi:10.1016/S0304-3800(03)00070-X.

Pessoa, S.P.M., Galvanin, E.A.d.S., Neves, S.M.A.d.S., 2014. Mapeamento do uso e ocupação da Floresta Aluvial no Rio Paraguai - Barra do Bugres/Mato Grosso. Revista Brasileira de Cartografia 66. URL: http://www.seer.ufu.br/index.php/revistabrasileiracartografia/article/view/44714.

QGIS Development Team, 2016. QGIS Geographic Information System. Open Source Geospatial Foundation Project. URL: http://qgis.osgeo.org.

Ribeiro, C.A.A.S., Soares, V.P., Oliveira, A.M.S., Gleriani, J.M., 2005. O desafio da delimitação de áreas de preservação permanente. Revista Árvore 29, 203 – 212. doi:10.1590/S0100-67622005000200004.

Ribeiro, H., Galvanin, E., Cocco, J., Dallacort, R., 2016. Characterizing the spatio-temporal land use in the Paraguai/Jauquara basin, Mato Grosso - Brazil. Revista Espacios 37.

Robertson, C., Nelson, T., Boots, B., Wulder, M., 2007. STAMP: Spatial-temporal analysis of moving polygons. Journal of Geographical Systems 9, 207–227. doi:10.1007/s10109-007-0044-2.

RStudio Team, 2019. RStudio: Integrated Development Environment for R. RStudio, Inc.. Boston, MA. URL: http://www.rstudio.com/.

Sadahiro, Y., Umemura, M., 2001. A computational approach for the analysis of changes in polygon distributions. Journal of Geographical Systems 3, 137–154. doi:10.1007/PL00011471.

Shao, F., Cai, S., Gu, J., 2010. A modified Hausdorff distance based algorithm for 2-dimensional spatial trajectory matching, in: 2010 5th International Conference on Computer Science Education, pp. 166–172.

Sohl, T., Dornbierer, J., Wika, S., Robison, C., 2019. Remote sensing as the foundation for high-resolution United States landscape projections – The Land Change Monitoring, assessment, and projection (LCMAP) initiative. Environmental Modelling & Software 120, 104495. URL: http://www.sciencedirect.com/science/article/pii/S1364815219303949, doi:10.1016/j.envsoft.2019.104495.

Sokal, R.R., Oden, N.L., 1978. Spatial autocorrelation in biology: 1. Methodology. Biological Journal of the Linnean Society 10, 199–228. doi:10.1111/j.1095-8312.1978.tb00013.x.

Souza, A., Mota, L., Zamadei, T., Martim, C.C., Almeida, F., Paulino, J., 2013. Classificação climática e balanço hídrico climatológico no estado de Mato Grosso. Nativa 01, 34–43. doi:10.14583/2318-7670.v01n01a07.

USGS, 2017. Aquisição de imagens orbitais digitais gratuitas do Satélite Landsat-8. URL: https://www.usgs.gov/core-science-systems/nli/landsat. (Accessed on 18 May 2018).

Veldkamp, A., Fresco, L., 1996. CLUE : a conceptual model to study the conversion of land use and its effects. Ecological modelling 85, 253–270. doi:10.1016/0304-3800(94)00151-0.

Verweij, P., Cormont, A., Kok, K., van Eupen, M., Janssen, S., Roller, J., de Winter, W., Pérez-Soba, M., Staritisky, I., 2018. Improving the applicability and transparency of land use change modelling: The iCLUE model. Environmental Modelling & Software 108. doi:10.1016/j.envsoft.2018.07.010.

Warra, H.H., Ahmed, M.A., Nicolau, M.D., 2015. Impact of land cover changes and topography on soil quality in the Kasso catchment, Bale Mountains of southeastern Ethiopia. Singapore Journal of Tropical Geography 36, 357–375. doi:10.1111/sjtg.12124.

Williams, E., Wentz, E., 2008. Pattern Analysis Based on Type, Orientation, Size, and Shape. Geographical Analysis 40, 97 – 122. doi:10.1111/j.1538-4632.2008.00715.x.

Xaud, M.R., Epiphanio, J.C.N., 2014. Dinâmica do uso e cobertura da terra no sudeste de Roraima utilizando técnicas de detecção de mudanças. Acta Amazonica 44, 107–120. doi:10.1590/S0044-59672014000100011.

Zhu, A.X., 1997. Measuring uncertainty in class assignment for natural resource maps under fuzzy logic. Photogrammetric Engineering and Remote Sensing 63, 1195–1201.